Particle swarm optimization-optimized integrator backstepping for the control of electric wheelchairs velocity

Djamila Boubekeur[1,2], Khayreddine Saidi[3,4], Mohammed Messirdi[3], Abdelmadjid Boumédiène[3]
[1]Department of Optics and Applied Physics, Institute of Science and Applied Technics, University of ORAN 1, Oran, Algeria
[2]Manufacturing Engineering Laboratory of Tlemcen, Tlemcen University, Tlemcen, Algeria
[3]Automatics Laboratory of Tlemcen, Department of Electrical and Electronic Engineering, Tlemcen University, Tlemcen, Algeria
[4]Department of Automatic Control, Faculty of Electrical Engineering, Djillali Liabes University, Sidi Bel Abbes, Algeria

Article Info

Article history:

Received Aug 27, 2025
Revised Oct 10, 2025
Accepted Oct 19, 2025

Keywords:

Electric powered wheelchair
Integrator backstepping control
Optimization
Particle swarm optimization
Permanent magnet synchronous motors

ABSTRACT

Most people suffering from temporary or permanent disabilities rely on wheelchairs or electric powered wheelchairs (EPW) to maintain autonomy of movement. To address different EPW control challenges, several studies have investigated this kind of robot. This paper focuses on the optimization of the integrator backstepping control parameters of the EPW. The system operates using two permanent magnet synchronous motors (PMSM), noted for their great efficiency, substantial torque, minimal noise, and robustness. At first, the dynamic model for both EPW-motors is showned. After that, a nonlinear integrator backstepping command based on Lyapunov's second technique, which combines the choice of the energy function with the control laws, was applied to the resulting global model. To ensure optimal performance, the control parameters were tuned by means of an optimization approach. Specifically, the particle swarm optimization technique (PSO) was employed to search for the optimal parameters (gains) of the integrator backstepping controller. In order to assess the performance of the optimized backstepping–based control approach, numerical simulations were conducted to illustrate the evolution of both electrical and mechanical velocity- related variables.

Corresponding Author:

Djamila Boubekeur
Department of Optics and Applied Physics, Institute of Sciences and Applied Physics
University of ORAN 1
Oran, Algeria
Email: djml.boubekeur@gmail.com

1. INTRODUCTION

Electric powered wheelchairs (EPWs) play a viral role in improving the autonomy and mobility of persons with severe motor impairments. As the global population ages and the incidence of neuromuscular disorders increases, the demand for intelligent, reliable, and user-friendly wheelchair systems continues to grow [1], [2]. Modern EPWs are expected not only to move users from one location to another but also to do so safely, smoothly, and with minimal effort, even in complex environments. Traditional joystick-based interfaces are often unsuitable for users with limited dexterity, prompting the development of autonomous or semi-autonomous control systems able to assist or replace manual operations [3]–[5].

To reach these requirements, various control strategies have been explored in order to improve EPW performance. They include proportional–integral–derivative (PID) control [6]–[8], fuzzy logic [9]–[11], neural networks [12], sliding mode control [13], [14], and nonlinear techniques like backstepping [15]–[17], to enhance the trajectory tracking, stability, and adaptability to users' changing habits and environment.

However, the effectiveness of these control systems is heavily dependent on the proper tuning of their parameters. Manually selecting control gains or thresholds is often inefficient, subjective, and unsuitable for real-time adaptation. Poorly tuned parameters can lead to sluggish response, instability, or excessive energy consumption, compromising both users' safety and comfort. To overcome these limitations, algorithms such as genetic algorithms (GA), particle swarm optimization (PSO) [18], and differential evolution (DE) were applied to optimize control parameters in EPWs, allowing for a systematic improvement of performance indices such as tracking accuracy, smoothness, control effort, and robustness [17], [19], [20]. On the other hand, machine learning methods, particularly neural networks and reinforcement learning, are developed to improve decision-making and system adaptability to users' preferences [21]. These approaches enable dynamic updates of controller parameters based on real usage conditions, thereby making EPWs sensitive and efficient in diverse environments [22].

The main objective of this study is to optimize the integrator backstepping control parameters for EPWs by integrating a metaheuristic optimization algorithm such as PSO. Inspired by animal social habits and behaviors, such as bird flocking, insect swarming, and fish schooling [23], [24]. In general, birds, insects, fish, and other animals always travel in groups wher their positions and velocities are adjusted according to information collected from the group. This technique enables individuals to reduce their own effort in tasks such as seeking shelter or food and avoiding predators.

After the introduction section, the paper presents two other sections. Section 2 covers the dynamic modelling of EPWs based on permanent magnet synchronous motors (PMSM) actuator and integrator backstepping control applied to the global system. After that, the PSO algorithm is applied to adjust the control parameters in order to improve the tracking trajectory and disturbance rejection. To achieve the study approach, simulation results are given in the final section.

2. MODELING AND PROPOSED METHOD

In this section, the experiment is processed with the method of modeling an electrically powered wheelchair described in [15], [25]. The chair has two stabilizing free wheels and two drive wheels, facilitating its displacement by means of their differential movements. The wheelchair is powered by two permanent magnet synchronous motors fed by two voltage inverters.

$$\begin{cases} \dot{x}_1 = x_2 \\ \dot{x}_2 = l_1 x_2 + l_2 x_4 + y_1 p\left[\left(L_{dr} - L_{qr}\right) x_5 x_7 + \phi_f x_7\right] + y_2 p\left[\left(L_{dl} - L_{ql}\right) x_6 x_8 + \phi_f x_8\right] + \frac{R}{a+b} T \\ \dot{x}_3 = x_4 \\ \dot{x}_4 = l_3 x_2 + l_4 x_4 + y_3 p\left[\left(L_{dr} - L_{qr}\right) x_5 x_7 + \phi_f x_7\right] + y_4 p\left[\left(L_{dl} - L_{ql}\right) x_6 x_8 + \phi_f x_8\right] + \frac{R}{a+b} T \\ \dot{x}_5 = -\frac{R_s}{L_{dr}} x_5 + p\Omega_r \frac{L_{qr}}{L_{dr}} x_7 + \frac{1}{L_{dr}} V_{dr} \\ \dot{x}_6 = -\frac{R_s}{L_{dl}} x_6 + p\Omega_l \frac{L_{ql}}{L_{dl}} x_8 + \frac{1}{L_{dl}} V_{dl} \\ \dot{x}_7 = -p\Omega_r \frac{L_{dr}}{L_{qr}} x_5 - \frac{R_s}{L_{qr}} x_7 + \frac{1}{L_{qr}} V_{qr} - \frac{p\Omega_r}{L_{qr}} \phi_f b \\ \dot{x}_8 = -p\Omega_l \frac{L_{dl}}{L_{ql}} x_6 - \frac{R_s}{L_{ql}} x_8 + \frac{1}{L_{ql}} V_{ql} - \frac{p\Omega_l}{L_{ql}} \phi_f \end{cases} \quad (1)$$

with:

$l_1 = l_4 = -\frac{ac}{a^2-b^2}$

$l_2 = l_3 = \frac{bc}{a^2-b^2}$

$y_1 = y_4 = \frac{aR}{a^2-b^2}$

$y_2 = y_3 = \frac{-bR}{a^2-b^2}$ and

$a = \frac{1}{\sigma} J_a + \sigma \left\{ J_w + \left(\frac{M}{4} + m_w\right) R^2 + \left(\frac{r}{L}\right)^2 J \right\}$

$b = \sigma R^2 \left(\frac{M}{4} - \frac{1}{L^2} J\right)$

$c = \frac{1}{\sigma} C_a + \sigma C_w$

$T = \sigma \left(\frac{M}{2} + m_w\right) gRsin\psi \begin{bmatrix} 1 \\ 1 \end{bmatrix}$

In this case, the chosen model motor of the PMSM with the round rotor (rotor surface magnets) was with a vector control. The presented model allowed a simple input system. Consequently, the applied control became easier, and $\dot{x}_5$ and $\dot{x}_6$ were equal to zero. The first inputs (right, left) are defined by:

$$V_{dr} = p\Omega_r L_{qr} x_7 \quad (2)$$

$$V_{dl} = p\Omega_l L_{ql} x_8 \quad (3)$$

The EPW parameters are given in Table 1.

Table 1. EPW parameters

Symbol	Descriptions	Value
v	Longitudinal velocity	*m/s*
α_r, α_l	Rotational angle of the right/left wheel	*rad*
α_{mr}, α_{ml}	Rotational angle of the right/left motor	*rad*
C_{emr}, C_{eml}	Electromagnetic torques of the right/left motor	*N.m*
C_r, C_l	Required load torques of the right/left motor	*N.m*
C_{Fr}, C_{Fl}	Torque applied on the right/left wheel	*N.m*
Ω_r, Ω_l	Angular rotor velocities of the right/left motor	*rad/s*
I_d, I_q	d- and q-axis stator currents	*A*
V_d, V_q	d- and q-axis stator voltages	*V*
M	EPW with operator mass	210 kg
m_w	Mass of driving wheel	2 kg
L	Distance between the two driving wheels	0.57 m
R	Radius of the driving wheel	0.17 m
J	Inertia moment of the EPW	16.08 $kg.m^2$
J_w	Moment of inertia of the driving wheel	0.0289 $kg.m^2$
g	Acceleration due to gravity	9.81 $\frac{m}{s^2}$
ψ	Slope angle	10 %
f_w	Viscous friction coefficient of the wheel	0.008 $N.m.s/rad$
σ	Gear ratio	0.01
J_a	Moment of inertia of the motor	0.0008 $kg.m^2$
f_v	Viscous friction coefficient of the motor	0.00005 $N.m.s/rad$
R_s	Per phase stator resistance	2.56 Ω
L_d	d-axis stator inductances	0.0064 H
L_q	q-axis stator inductances	0.0056 H
φ_f	Permanent magnet flux	0.06 Wb
P	Pair number of poles	4
P_n	Rated power	400 W
I_n	Current	4 A
N_n	Rated speed	3000 rpm

2.1. Integrator backstepping control

The backstepping control approach is based on Lyapunov's second technique, which combines control laws and energy function choice. The controller is not only responsible for achieving its intended goal, whether tracking and/or regulation, but it must also guarantee at all times that, the compensated system remains globally asymptotically stabe. Backstepping is a step-by-step design method rooted in Lyapunov's stability theory, where each state is introduced progressively as a virtual control input to stabilize its corresponding subsystem [25].

Integrating an integral action within backstepping-based control laws constitutes a widely adopted strategy to enhance the robustness of the approach, ensuring the rejection of disturbances and the attenuation of steady-state tracking errors. The bloc diagram of integrator backstepping control for EPW is presented in Figure 1. The steps followed for the synthesis of the speed controller can be outlined as follows:

– Step 1: Right wheel speed control

First, the tracking objective defines the tracking error for the right wheel speed as (4)

$$e_1 = x_2 - x_{2ref} + k_{x2} \int_0^t \left(x_2 - x_{2ref}\right) dt \quad (4)$$

The Lyapunov law considered and its derivate are:

$$V(e_1) = (1/2)e_1^2, \dot{V}(e_1) = e_1(\dot{x}_2 - \dot{x}_{2ref}) + k_{x2}(x_2 - x_{2ref})$$
$$= e_1\left(l_1x_2 + l_2x_4 + y_1Cem_{r\_ref} + y_2Cem_{l\_ref} + T - \dot{x}_{2ref} + k_{x2}(x_2 - x_{2ref})\right) \quad (5)$$

To obtain the negative derivate of Lyapunov function, the virtual control was considered as (6):

$$\varphi(e_1) = -C_1e_1 + \dot{x}_{1ref} \quad (6)$$

The torque control expression was obtained as (7):

$$y_1Cem_{r\_ref} + y_2Cem_{l\_ref} = -C_2e_1 - l_1x_2 - l_2x_4 - T - k_{x2}(x_2 - x_{2ref}) \quad (7)$$

with: $y_0 = -C_2e_1 - l_1x_2 - l_2x_4 - T - k_{x2}(x_2 - x_{2ref})$
Therefore: $\dot{V}(e_1) = -C_1e_1^2 < 0$
with $C_1 > 0$. Given that the theorem's conditions are satisfied; the stability of the first subsystem is ensured in the sense of asymptotic convergence.

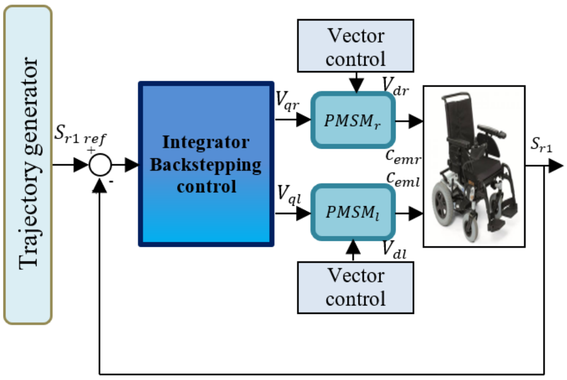

Figure 1. Bloc diagram of integrator backstepping control for EPW

– Step 2: Left wheel speed control

For the left wheel speed, the tracking objective is formulated by introducing the tracking error, defined as follows:

$$e_2 = x_4 - x_{4ref} + k_{x4}\int_0^t (x_4 - x_{4ref})dt \quad (8)$$

x_{4ref} corresponds to the previous virtual control $\varphi(e_1)$
The increased energy function, together with its time derivative, are defined as follows:

$$V(e_1, e_2) = 1/2e_1^2 + 1/2\,e_2^2, \dot{V}(e_1, e_2) = e_1\dot{e}_1 + e_2\dot{e}_2$$
$$e_2\dot{e}_2 = e_2\left(\dot{x}_4 - \dot{x}_{4ref} + k_{x4}(x_4 - x_{4ref})\right) \quad (9)$$

$$= l_3x_2 + l_4x_4 + y_3Cem_{r\_ref} + y_4Cem_{l\_ref} + T - \dot{x}_{4ref} + k_{x4} \quad (10)$$

The torque control expression was obtained:

$$y_3Cem_{r\_ref} + y_4Cem_{l\_ref} = -C_4e_2 - l_3x_2 - l_4x_4 - T - k_{x4}(x_4 - x_{4ref}) \quad (11)$$

with:

$$y_5 = -C_4e_2 - l_3x_2 - l_4x_4 - T - k_{x4}(x_4 - x_{4ref})$$

Thus: $\dot{V}(e_1, e_2) = -C_1e_1^2 - C_2e_2^2 < 0$

With: $C_{1,2} > 0$, the stability properties of both subsystems were formally verified.
The unknown control system is summarized as:

$$\begin{cases} y_1 Cem_{r\_ref} + y_2 Cem_{l\_ref} = y_0 \\ y_3 Cem_{r\_ref} + y_4 Cem_{l\_ref} = y_5 \end{cases} \tag{12}$$

The reference input torques for the right and left wheels were derived by solving the final two equations, yielding:

$$Cem_{r\_ref} = y_0/y_1 - y_2/y_1 Cem_{l\_ref} \tag{13}$$

$$Cem_{l\_ref} = y_1 y_5 - y_3 y_0/y_4 y_1 - y_3 y_2 \tag{14}$$

– Step 3: Right wheel electromagnetic torque control
For this step, the error is defined as:

$$e_3 = Cem_r - Cem_{r\_ref} + k_{x3}\int_0^t (Cem_r - Cem_{r\_ref})dt \tag{15}$$

$$\dot{e}_3 = C\dot{e}m_r - C\dot{e}m_{r\_ref} + k_{x3}\left(Cem_r - Cem_{r\_ref}\right) \tag{16}$$

The adopted Lyapunov function and its corresponding time derivative are given by:

$$V(e_1, e_2, e_3) = \frac{1}{2}e_1^2 + \frac{1}{2}e_2^2 + \frac{1}{2}e_3^2$$
$$\dot{V}(e_1, e_2, e_3) = e_1\dot{e}_1 + e_2\dot{e}_2 + e_3\dot{e}_3$$

The torque expression (rotor surface magnets) is formulated as (17).

$$Cem_r = P\varphi_f I_{qr} \tag{17}$$

By replacing (17) in (16)

$$\dot{e}_3 = P\varphi_f/L_d\left[\left(V_{qr} - R_s I_q - wL_d I_q - w\varphi_f\right) - C\dot{e}m_{r\_ref}\right] + k_{x3}(Cem_r - Cem_{r\_ref}) \tag{18}$$

The real input control of the right motor is:

$$V_{qr} = -C_5 e_5 + R_s I_{qr} + wL_d I_{dr} + w\varphi_f + (\frac{L_q}{P\varphi_f)} C\dot{e}m_{r\_ref} \tag{19}$$

with

$$C\dot{e}m_{r\_ref} = \frac{(1}{y_0)}\dot{y}_0 - \frac{(y_2}{y_1)} C\dot{e}m_{l\_ref}$$

and

$$\dot{y}_0 = [C_2(l_1 + k_{x2}) + l_1^2 + l_2 l_3 + l_1 k_{x2}]x_2 - [(C_2 + l_1 + l_4 + k_{x2})l_2]x_4 - [(C_2 + l_1 + k_{x2})y_1 + l_2 y_3]Cem_{r\_ref} - [(C_2 + l_1 + k_{x2})y_2 + l_2 y_4]Cem_{l\_ref} - [C_2 + l_1 + l_2 + k_{x2}]T$$

Therefore,

$$\dot{V}(e_1, e_2, e_3) = -C_1 e_1^2 - C_2 e_2^2 - C_3 e_3^2 < 0,\ C_{1,2,3} > 0$$

– Step: Left wheel electromagnetic torque control
Let e_4 denote the last error:

$$e_4 = Cem_l - Cem_{l\_ref} + k_{x4}\int_0^t (Cem_l - Cem_{l\_ref})\, dt \tag{20}$$

The final Lyapunov increased function and its derivative are:

$$V(e_1,e_2,e_3,e_4)=\frac{1}{2}e_1^2+\frac{1}{2}e_2^2+\frac{1}{2}e_3^2+\frac{1}{2}e_4^2$$
$$\dot{V}(e_1,e_2,e_3,e_4)=e_1\dot{e}_1+e_2\dot{e}_2+e_3\dot{e}_3+e_4\dot{e}_4$$
$$\dot{e}_4=\dot{Cem}_l-\dot{Cem}_{l\_ref}+k_{x4}(Cem_l-Cem_{l\_ref}) \quad (21)$$

The torque expression (rotor surface magnets) is rxpressed as follows:

$$Cem_l=P\varphi_f I_{ql} \quad (22)$$

By replacing (22) in (21).

$$\dot{e}_4=\frac{P\varphi_f}{L_d}\left[\left(V_{ql}-R_sI_q-wL_dI_q-w\varphi_f\right)-\dot{Cem}_{l\_ref}\right]+k_{x4}(Cem_l-Cem_{l\_ref})\ldots\ldots \quad (23)$$

The real input control:

$$V_{ql}=-C_4e_4+R_sI_q+wL_dI_d+w\varphi_f+\frac{L_q}{P\varphi_f}\dot{Cem}_{l\_ref}-\frac{L_q}{P\varphi_f}\left(k_{x4}(Cem_l-Cem_{l\_ref})\right) \quad (24)$$

with

$$\dot{Cem}_{r\_ref}=\frac{(1}{y_4y_1-y_3y_2)}(y_1\dot{y}_5-y_3\dot{y}_0)$$

and

$$\dot{y}_5=[(C_4+l_1+l_4+k_{x2})l_3]x_2-[C_4(l_4+k_{x4})+l_4^2+l_2l_3+l_4k_{x4}]x_4-[(C_4+l_4+k_{x3})y_3+l_3y_1]Cem_{r\_ref}-[(C_4+l_4+k_{x4})y_4+l_2y_3]Cem_{l\_ref}-[C_4+l_4+l_3+k_{x4}]T$$

Therefore,

$$\dot{V}(e_1,e_2,e_3,e_4)=-C_1e_1^2-C_2e_2^2-C_3e_3^2-C_4e_4^2<0$$

Take $C_{1,2,3,4}>0$.
The system's second control input $V_{dr,l}$ was determined using the PMSM vector control to eliminate the coupling input of the system by maintaining I_d equal to zero. The gains $C_{1,2,3,4}$ and $k_{x1,2,3,4}$acts a damping terms that stabilized the dynamics of error variable $e_{1,2,3,4}$, and minimized or eliminated the static error.

3. METHOD

The PSO algorithm refers to each element as a particle and the population as a swarm. Using particle and group memory to search for optimization in the solution space is the main idea underlying this approach. It also produces a very high probability of convergence of the optimization objective function to the global optimal solution. This property of the PSO underlies the algorithm's significant impact in addressing combinatorial and nonlinear optimization problems [18], [19].

The movement of each particle in the search space depends on the best-explored places of both its finding and the whole swarm, respectively, which are called pbest and gbest. For the purpose of updating pbest and gbest, each particle collects and stores information in a vector to be analyzed [23].

A population of random solutions was used to initialize the "swarm" where each particle (for example, the l^{th} particle) has a position coordinate and a corresponding velocity, denoted respectively $x_l=(x_{l1},x_{l2},\ldots\ldots x_{lN})$ and $v_l=(v_{l1},v_{l2},\ldots\ldots v_{lN})$ for N-dimensional space.

The efficiency of a solution can be measured through a fitness function, which evaluates the quality of each particle's position. Accordingly, one can store the $pbest$ of particle l, represented by $pbest_l=(pbest_{l1},pbest_{l2},\ldots\ldots pbest_{lN})$, and the $gbest$, represented by $gbest=(gbest_1,gbest_2,\ldots\ldots gbest_N)$.

The following (25) and (26) represent how the algorithm updates the particle positions and velocities shown in Figure 2 at each iteration of the optimization process, utilizing the previous information:

$$v_l(i)=w*v_l(i-1)+r_1\varphi_1*\left(pbest_l-x_l(i-1)\right)+r_2\varphi_2*\left(gbest-x_l(i-1)\right) \quad (25)$$

$$x_l(i)=x_l(i-1)+v_l(i) \quad (26)$$

where w represents the inertia weight, which controls how the direction of displacement affects subsequent displacement, where r_1 and r_2 are random numbers in the interval [0, 1]. Acceleration constants φ_1 and φ_2 control the particle's cognitive behavior and social aptitude, respectively. Both of these parameters are positive and provided empirically in accordance with the relationship $\varphi_1 + \varphi_2 \leq 4$.

Figures 2 and 3 present the particle movement schematic in the PSO and the algorithm flowchart, respectively. As aforementioned, each particle retains a memory of its earlier best position indicated as pbest, and global best position reached by the particles of the swarm, given as gbest [23].

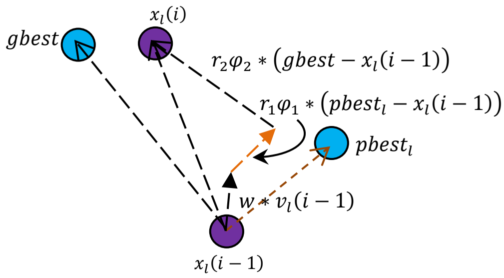

Figure 2. Particle movement schematic in the PSO

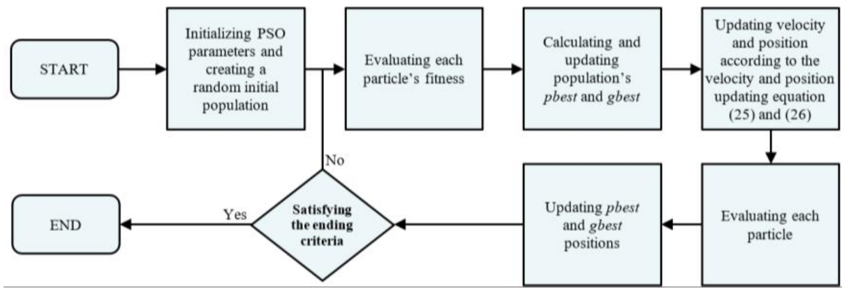

Figure 3. PSO algorithm flowchart

In this work, the squared error-based fitness function was defined and expressed by (27).

$$fitness = \sum_{i=1}^{N} e(i)^2 = \sum_{i=1}^{N} error^2 \quad (27)$$

here $e(i)$ denotes the trajectory error of the i^{th} sample, and N represents the number of the sample. The proposed optimized control scheme is illustrated in Figure 4.

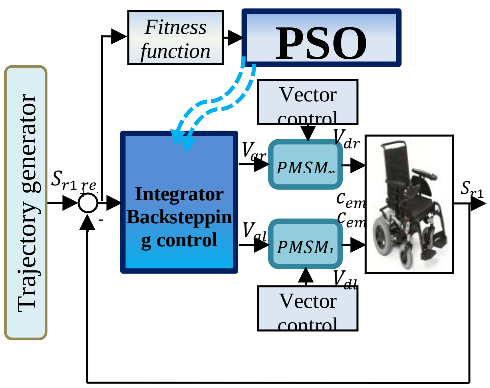

Figure 4. The proposed optimized control scheme

4. RESULTS AND DISCUSSION

To evaluate the performance of the control applied to EPW driven by two PMSMs, the velocity tracking was simulated by using the PSO parameters determined through a series of experiments demonstrated by Table 2. The optimal gain values determined are summarized in Table 3. The worst-case scenario that the EPW operator can face was chosen. The trajectory considered during the simulation is described as follows: the EPW is on slope $\psi = 10°$. There are two turns: one to the right, which occurs at $t = 13$ s, and the next to the left occurring at $t = 17$ s. Both are followed by braking after $t = 20$ s. The speed reference is generated using a hyperbolic tangent profile to guarantee smooth transitions and continuity between successive reference values.

Table 2. PSO parameters for integrator backstepping controller

Parameters	Value
Cognitive constant (φ1)	2
Group constant (φ2)	2
Inertia weight (w)	0.5
Number of particles (np)	40
Number of iteration (nit)	100

Table 3. The best gain values

Parameters	Value
C1	110
C2	5
C3	108.0384
C4	20
Kx1	957.8562
Kx2	100
Kx3	1100
Kx4	110

Figure 5 represents the velocity trajectory tracking of the right and left drive wheels. It is worth noting that the measured speeds follow perfectly the references without overshoot. The response time is 9.29 s and static error is 7×10^{-3}. The velocities increase to a nominal value, which is maintained during the slope, and then return to zero. This corresponds to the braking. Figure 6 illustrates the evolution of the electromagnetic torque $Cem_{r,l}$ of both PMSMs. When the wheelchair moves straight, even in the presence of a slope, the left and right torques have the same value and increase proportionally with the speed. When a change of direction occurs, the left and right torques react in opposite ways in order to steer the wheelchair, then return to the same value once the turn is completed. Afterward, a speed degradation appears until the wheelchair eventually stops on the slope, which explains the final torque value of 1 Nm. These torques are directly proportional to the stator quadrature currents $I_{qr,l}$ as illustrated in Figure 7. The stator direct currents $I_{dr,l}$ are maintained at zero through vector control, as depiced in Figure 8. The direct and quadrature voltage inputs of both PMSMs $(V_{dr,l}, V_{qr,l})$ remain within their nominal values as shown in Figures 9 and 10, respectively. The Phase-a stator voltage and Phase-a stator current are shown in Figures 11 and 12, respectively.

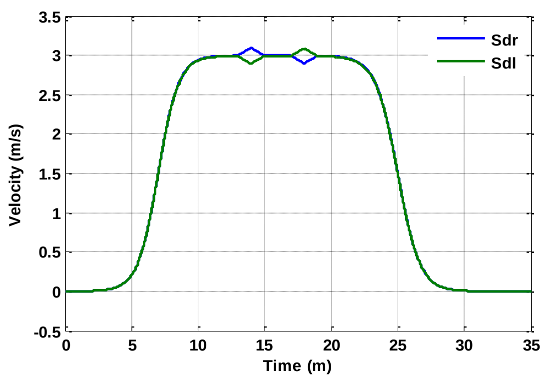

Figure 5. Right/left wheel velocity

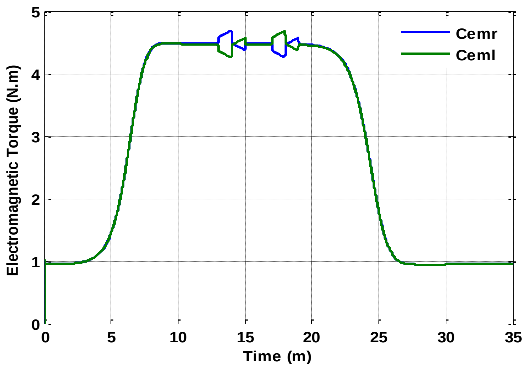

Figure 6. The right/left electromagnetic torque

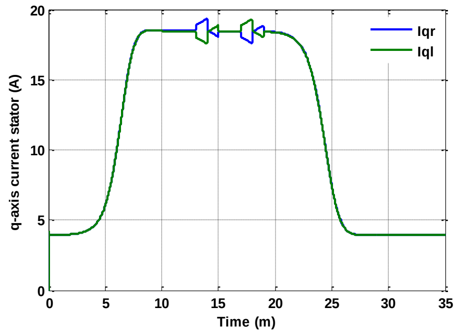

Figure 7. The right/left q-axis current stator

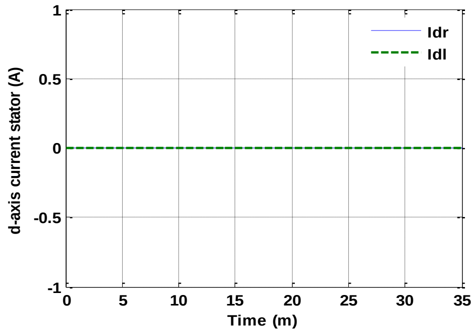

Figure 8. The right/left d-axis current stator

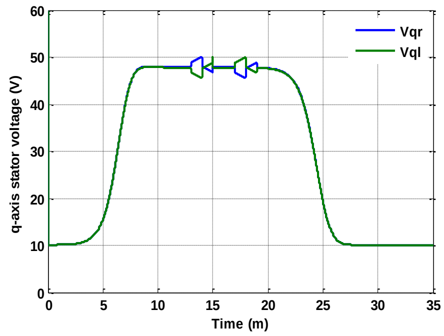

Figure 9. The right/left q-axis stator voltage

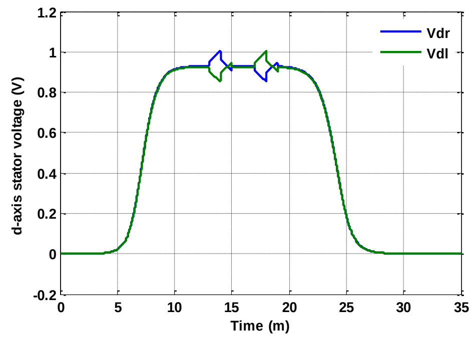

Figure 10. The right/left d-axis stator voltage

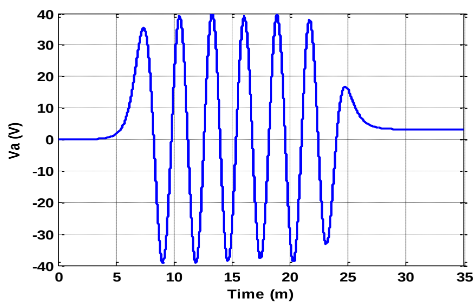

Figure 11. Phase-a stator voltage

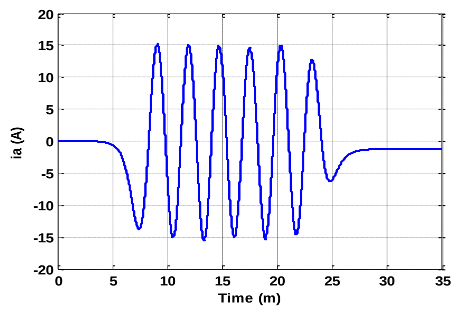

Figure 12. Phase-a stator current

5. CONCLUSION

The application of an optimal PSO algorithm to the integrator backstepping velocity control of an electrically powered wheelchair facilitated effective adjustment of the control parameters, thereby improving trajectory tracking and disturbance rejection. Simulation results confirmed that the suggested controller is able to achieve smooth, accurate, and stable velocity tracking, which in turn improves maneuverability and user safety.

ACKNOWLEDGMENTS

This work is supported by the General Directory of Scientific Research and Technological Development (DG RSDT).

FUNDING INFORMATION

Authors state no funding involved.

AUTHOR CONTRIBUTIONS STATEMENT

This journal uses the Contributor Roles Taxonomy (CRediT) to recognize individual author contributions, reduce authorship disputes, and facilitate collaboration.

Name of Author	C	M	So	Va	Fo	I	R	D	O	E	Vi	Su	P	Fu
Djamila Boubekeur	✓	✓	✓	✓	✓	✓	✓	✓	✓	✓	✓	✓	✓	
Khayreddine Saidi		✓	✓	✓			✓	✓	✓	✓	✓	✓		
Mohammed Messirdi		✓		✓						✓	✓	✓		
Abdelmadjid Boumediène	✓	✓		✓			✓			✓	✓	✓		✓

C : **C**onceptualization
M : **M**ethodology
So : **So**ftware
Va : **Va**lidation
Fo : **Fo**rmal analysis
I : **I**nvestigation
R : **R**esources
D : **D**ata Curation
O : Writing - **O**riginal Draft
E : Writing - Review & **E**diting
Vi : **Vi**sualization
Su : **Su**pervision
P : **P**roject administration
Fu : **Fu**nding acquisition

CONFLICT OF INTEREST STATEMENT

Authors state no conflict of interest.

DATA AVAILABILITY

Data availability is not applicable to this paper as no new data were created or analyzed in this study.

REFERENCES

[1] G. Bourhis, O. Horn, O. Habert, and A. Pruski, "An autonomous vehicle for people with motor disabilities," *IEEE Robotics & Automation Magazine*, vol. 8, no. 1, pp. 20–28, Mar. 2001, doi: 10.1109/100.924353.

[2] S. P. Parikh, V. Grassi, V. Kumar, and J. Okamoto, "Integrating human inputs with autonomous behaviors on an intelligent wheelchair platform," *IEEE Intelligent Systems*, vol. 22, no. 2, pp. 33–41, Mar. 2007, doi: 10.1109/MIS.2007.36.

[3] J. Cui, Y. Shang, S. Yu, and Y. Wang, "Research on intelligent wheelchair multimode human–computer interaction and assisted driving technology," *Actuators*, vol. 13, no. 6, p. 230, Jun. 2024, doi: 10.3390/act13060230.

[4] H. Iqbal, J. Zheng, R. Chai, and S. Chandrasekaran, "Electric powered wheelchair control using user-independent classification methods based on surface electromyography signals," *Medical & Biological Engineering & Computing*, vol. 62, no. 1, pp. 167–182, Jan. 2024, doi: 10.1007/s11517-023-02921-z.

[5] W. Meddeber, B. Aour, and K. Labadi, "Smart wheelchair localization and navigation based on multi-sensor data fusion using hybrid-filter method (HF)," *Revue d'Intelligence Artificielle*, vol. 38, no. 2, pp. 387–396, Apr. 2024, doi: 10.18280/ria.380202.

[6] N. Thongpance *et al.*, "Comparative analysis of PID tuning methods for speed control in Mecanum-wheel electric wheelchairs," *Buletin Ilmiah Sarjana Teknik Elektro*, vol. 7, no. 2, pp. 95–110, 2025.

[7] R. Chotikunnan, P. Chotikunnan, N. Thongpance, T. Puttasakul, Y. Pititheeraphab, and M. Sangworasil, "Application of PID control system in Mecanum wheelchair," *International Journal of Membrane Science and Technology*, vol. 10, no. 3, pp. 3519–3529, Aug. 2023, doi: 10.15379/ijmst.v10i3.3395.

[8] W. Yu, W. Dazhi, and Z. Yufeng, "Intelligent wheelchair obstacle avoidance design based on fuzzy PID control," *Journal of Shanghai University of Engineering Science*, vol. 38, no. 3, pp. 250–256, 2024.

[9] M. Mohammed, B. Abdelmadjid, and B. Djamila, "Comparative study between integrator backstepping and fuzzy logic control applied to an electric powered wheelchair," *European Journal of Electrical Engineering*, vol. 23, no. 3, pp. 165–174, Jun. 2021, doi: 10.18280/ejee.230301.

[10] S. Sumardi, A. Sofwan, A. Hidayatno, and A. Patadani, "Wheelchair speed adjustment based on fuzzy logic controller for user comfort," *International Journal of Engineering and Information Systems (IJEAIS)*, vol. 5, no. 10, pp. 63–72, 2021.

[11] E. Yulianto, U. M. U. Salwa, T. Triwiyanto, and T. B. Indarto, "Wheelchair safety system using fuzzy logic controller to avoid obstruction," *International Journal of Electrical and Computer Engineering (IJECE)*, vol. 14, no. 6, pp. 7001–7012, Dec. 2024, doi: 10.11591/ijece.v14i6.pp7001-7012.

[12] K. Anam *et al.*, "Electroencephalography-based wheelchair navigation control using convolutional neural network method," *TELKOMNIKA (Telecommunication Computing Electronics and Control)*, vol. 23, no. 1, pp. 147–155, Oct. 2024, doi: 10.12928/telkomnika.v23i1.25988.

[13] M. Bakouri *et al.*, "Robust dynamic control algorithm for uncertain powered wheelchairs based on sliding neural network approach," *AIMS Mathematics*, vol. 8, no. 11, pp. 26821–26839, 2023, doi: 10.3934/math.20231373.

[14] P. S. Yadav, V. Agrawal, J. C. Mohanta, and M. D. Faiyaz Ahmed, "A robust sliding mode control of mecanum wheel-chair for trajectory tracking," *Materials Today: Proceedings*, vol. 56, pp. 623–630, 2022, doi: 10.1016/j.matpr.2021.12.398.

[15] M. Mohammed, B. Abdelmadjid, and B. Djamila, "A fuzzy logic controller for electric powered wheelchair based on lagrange model," *2019 International Conference on Advanced Electrical Engineering (ICAEE). IEEE*, pp. 1–6, Nov. 2019, doi: 10.1109/icaee47123.2019.9014838.

[16] M. Jiang, L. Chen, Y. Wang, and H. Wu, "Adaptive backstepping control for Mecanum-wheeled omnidirectional vehicle using neural networks," *IEEJ Transactions on Electrical and Electronic Engineering*, vol. 17, no. 3, pp. 378–386, Mar. 2022, doi: 10.1002/tee.23521.

[17] M. Kosaka and H. Nakamura, "Backstepping CBF design for collision avoidance of electric wheelchair," *IFAC-PapersOnLine*, vol. 56, no. 1, pp. 331–336, 2023, doi: 10.1016/j.ifacol.2023.02.056.

[18] J. Kennedy and R. Eberhart, “Particle swarm optimization,” in *International Conference on Neural Networks*, 1995.

[19] A. M. Hamed, A.-F. Attia, and H. El-Behery, “Optimization of EEG-based wheelchair control: machine learning, feature selection, outlier management, and explainable AI,” *Journal of Big Data*, vol. 12, no. 1, Jul. 2025, doi: 10.1186/s40537-025-01238-y.

[20] M. Turki and A. Sakly, “Modelling of water level system using neurofuzzy tuned by PSO,” in *2016 17th International Conference on Sciences and Techniques of Automatic Control and Computer Engineering (STA)*, Dec. 2016, pp. 54–60, doi: 10.1109/STA.2016.7952055.

[21] K. Mistry, L. Zhang, S. C. Neoh, C. P. Lim, and B. Fielding, “A micro-GA embedded PSO feature selection approach to intelligent facial emotion recognition,” *IEEE Transactions on Cybernetics*, vol. 47, no. 6, pp. 1496–1509, Jun. 2017, doi: 10.1109/TCYB.2016.2549639.

[22] A. Amrane and Y. Zennir, “Trajectory tracking control of an autonomous electric wheelchair using particle swarm optimization based PID controller,” in *2023 IEEE 11th International Conference on Systems and Control (ICSC)*, Dec. 2023, pp. 731–736, doi: 10.1109/ICSC58660.2023.10449759.

[23] K. Saidi, A. Boumediene, and S. Massoum, “An optimal PSO-based sliding-mode control scheme for the robot manipulator,” *Elektrotehniski Vestnik/Electrotechnical Review*, vol. 87, no. 1–2, pp. 53–59, 2020.

[24] J. Sun, P. Zhang, and X. Kong, “Wireless sensor node localization algorithm combined with PSO-DFP,” *Journal of Intelligent Systems*, vol. 32, no. 1, Sep. 2023, doi: 10.1515/jisys-2022-0323.

[25] H. M. Shim, J. P. Hong, S. B. Chung, and S. H. Hong, “A powered wheelchair controller based on master-slave control architecture,” in *ISIE 2001. 2001 IEEE International Symposium on Industrial Electronics Proceedings (Cat. No.01TH8570)*, 2001, vol. 3, pp. 1553–1556, doi: 10.1109/ISIE.2001.931937.

BIOGRAPHIES OF AUTHORS

Djamila Boubekeur possesses an Engineering Degree in Electronics and a Magister Degree in Automatics delivered in 2007 and 2009, respectively by the University of Tlemcen, Algeria. She obtained her Ph.D. in Automatic Control Engineering in 2016, delivered by the same university. She has been a member of MELT laboratory since 2010. Since 2017, she has been working as a lecturer at the Optics and Applied Physics Department of ISTA (Institute of Sciences and Applied Physics) at the University of ORAN 1, Algeria. Her research interests concern modelization and control in robotics applications, robust control, artificial intelligence (fuzzy logic, genetic algorithm, PSO) and optimization. She can be contacted at email: djml.boubekeur@gmail.com.

Khayredine Saidi possesses an Engineering Degree in Automatic Control delivered by University of Tlemcen, Algeria. He received the Magister’s degree in Automatic Control Engineering, Robotics and Manufacturing Engineering from the University of Sciences and Technology of Oran (Algeria), in 2009. He obtained his Ph.D. in Automatic Control Engineering in 2021 delivered by University of Tlemcen, Algeria. He joined the Automatic Department of Tizi Ouzou University, Algeria in 2010. Since 2015 he teaches at the Electrical Engineering Faculty, Sidi Bel Abbes University, Algeria. His research interest’s concern: modelisation and control in robotics applications, robust control, artificial intelligence (fuzzy logic, genetic algorithm, PSO) and optimisation. Correspondence address: Automatic Department, Electrical Engineering Faculty, Sidi Bel Abbes University, Algeria. He can be contacted at email: saidi_kheiro@yahoo.fr.

Mohammed Messirdi received the Engineer degree in Automatic Control Engineering from the Tlemcen University, Algeria, in 2005. He received the Magister degree in Electronique, Signals and Systems, and the Ph.D. degree in Automatic Control Engineering from the University of Tlemcen, Algeria, in 2009 and 2025, respectively. He is LAT laboratory member since 2013. His research interest’s concern: linear and nonlinear hinfinity control and observer. He can be contacted at email: medauto3@gmail.com.

Abelmadjid Boumédiène received the Engineer degree in Electrotechnics, the Magister’s degree and Ph.D. in Electrical Engineering, from the Ecole Nationale Polytechnique (E.N.P), Algiers, Algeria, in 1991, 1994 and 2007 respectively. Upon graduation, he joined the Electrical Engineering Department of University of Bechar. He was an associate Professor, member of Process Control Laboratory (ENP). Since 2012, he joined the Electrical Engineering Department of University of Tlemcen. He is an associate Professor, member of Automatique Laboratory of Tlemcen (LAT). His research interests include electric machine drives, power electronics and process control. He can be contacted at email: a10boumediene@yahoo.fr.